NASA TECHNICAL NOTE

NASA TN D-6168

THE GAS PHASE IN POROUS FUEL-CELL ELECTRODES

by Robert W. Easter

Lewis Research Center
Cleveland, Ohio 44135

NATIONAL AERONAUTICS AND SPACE ADMINISTRATION • WASHINGTON, D. C. • FEBRUARY 1971

1. Report No.	2. Government Accession No.	3. Recipient's Catalog No.
NASA TN D-6168		

4. Title and Subtitle	5. Report Date
THE GAS PHASE IN POROUS FUEL-CELL ELECTRODES	February 1971
	6. Performing Organization Code

7. Author(s)	8. Performing Organization Report No.
Robert W. Easter	E-5754
	10. Work Unit No. 120-34

9. Performing Organization Name and Address	11. Contract or Grant No.
Lewis Research Center National Aeronautics and Space Administration Cleveland, Ohio 44135	

12. Sponsoring Agency Name and Address	13. Type of Report and Period Covered
National Aeronautics and Space Administration Washington, D. C. 20546	Technical Note
	14. Sponsoring Agency Code

15. Supplementary Notes

16. Abstract

A generalized physical model of a porous fuel-cell electrode is described, and the basic equations pertaining to the gas phase therein are presented. The equations are solved for various postulated spatial distributions of current production in the electrode. Three dimensionless parameters are defined, the numerical values of which yield information about the concentration gradients in the gas phase within the electrode for both pure reactant gases and reactant gases containing an inert impurity.

17. Key Words (Suggested by Author(s))	18. Distribution Statement
Fuel cells; Porous electrodes; Gas phase; Mass transport; Concentration gradients; Impurity buildup; Reactants	Unclassified - unlimited

19. Security Classif. (of this report)	20. Security Classif. (of this page)	21. No. of Pages	22. Price*
Unclassified	Unclassified	44	$3.00

*For sale by the National Technical Information Service, Springfield, Virginia 22151

CONTENTS

THE GAS PHASE IN POROUS FUEL-CELL ELECTRODES

by Robert W. Easter

Lewis Research Center

SUMMARY

A generalized physical model of a porous fuel-cell electrode has been presented which does not require postulation of any particular geometrical configuration. This allows the writing of the basic conservation equations describing the electrode in relatively simple general forms.

Applying the equations in a number of situations shows that the composition of the gas phase in fuel-cell electrodes is dependent on the values of the three parameters J, θ, and φ, where

$$J = \frac{\tau I_{vol} L}{n_R f C_T D_{H_2O\text{-}R} \epsilon \, \delta A};$$

$$\theta = \frac{D_{I\text{-}R}}{D_{I\text{-}H_2O}}; \text{ and}$$

$$\varphi = \frac{D_{I\text{-}R}}{D_{H_2O\text{-}R}}$$

τ is electrode tortuosity, I_{vol} is total current produced by electrode volume element, L is z-value of greatest penetration of gas phase toward bulk electrolyte, n_R is equivalents per gram-mole or reactant, f is Farraday's constant (9.65×10^{-4} A-sec/g-equiv), C_T is total concentration, ϵ is ratio of cross-sectional area to geometric cross-sectional area, and δA is increment of electrode surface area. The quantity J may be thought of as a dimensionless current density, while θ and ϕ are ratios of binary-gas-phase diffusion coefficients. The significance of these parameters is that for many purposes they make detailed analysis unnecessary. Considerable information is given simply by the magnitude of the parameters.

In particular, criteria are established whereby it can be determined whether gas-phase concentration gradients within the electrodes are significant. The parameters are also related to the accumulation of gaseous inert impurities in the electrode.

INTRODUCTION

Vital to the operation of porous fuel-cell electrodes are large amounts of gas-liquid and liquid-solid interfacial area in close proximity to each other. Thus, understanding of fuel-cell operation requires knowledge of the processes going on in all three phases: gas, liquid, and solid. Because of the interaction of these processes, any description of fuel-cell operation is of necessity quite complicated. A further hindrance to understanding is the fact that only overall performance may be investigated experimentally for most electrodes.

Although a number of fairly complex mathematical models of the operation of porous fuel-cell electrodes exist (see refs. 1 and 2 for summaries) none of these consider the gas phase within the electrode in any detail. This neglect is due chiefly to the complexity of porous electrode behavior. It is difficult enough to describe kinetic and liquid-phase phenomena, without coupling possible gas-phase effects.

In this work, however, an attempt is made to shed some light on the state of the gas phase in operating electrodes. In order to focus on the gas phase, and to avoid complexity, the following approach was taken:

(1) Establish a generalized physical picture which can be analysed in an orderly manner.

(2) Present the basic gas-phase conservation equations which apply to the established picture.

(3) Obtain the specific forms of these equations that apply to specific electrode types.

(4) Solve the specific equations and draw suitable general conclusions from the results.

Rather than solve simultaneously the analogous equations describing the liquid and solid phases in the electrode, reasonable forms for the liquid- and solid-phase phenomena are postulated.

While an approach of this nature usually limits the confidence with which results may be applied in cases which differ from those considered, it will be shown that several characteristics appear consistently, regardless of the specifics of a particular case. Furthermore, the first two sections of this report, corresponding to points (1) and (2) in the preceding list, are quite general and form a useful basis for analyzing the gas phase in any electrode.

There are several ways in which the information generated by analysis of the gas phase is useful:

(1) In the construction of complete models of electrode behavior, simplifying assumptions regarding the gas phase may be made more intelligently. It is possible to determine, for instance, the conditions under which concentration gradients are approximately linear, or negligible.

(2) The consequences of impure fuels and oxidant may be assessed.

(3) The effects of the bulk gas in the gas cavity on the electrode interior are more recognizable.

GENERALIZED PHYSICAL MODEL OF ELECTRODE INTERIOR

To analyse the mass transfer characteristics of a porous fuel-cell electrode it is necessary to establish an idealized picture of the electrode interior. If the results of the analysis are to have wide application, the picture or model adopted should be as general as possible. Thus, the parameters to which the model gives rise, while being few in number, should have meaning regardless of the specific electrode under consideration. To this end, consider a cylindrical section "punched out" of an operating electrode in a fuel cell, with a diameter large with respect to the mean diameter of the particles of which it is constructed, but small with respect to the overall electrode measurements (see fig. 1). The volume of this cylinder will be filled with solid material (catalyst; support structure), liquid, and gas. Current is produced at sites on the solid surfaces which (1) are catalytic in nature, (2) are immersed in liquid which is continuously connected by a liquid path to liquid covering a similar site in the other electrode, (3) are connected by an electronic path to active sites in the other electrode, (4) are relatively near an area of gas-liquid interface. The liquid will consist of a solvent which may take part in the electrode reaction, charged species which may appear or disappear at reaction sites and dissolved gases. The gas phase will be made up of reactants supplied externally, vapor of the volatile liquid species, and possibly other species present as impurities in the reactant supplied.

The bulk or net movement of the reactant gas in the electrode will be in a direction away from the gas cavity and normal to the electrode face. The twisting and turning nature of that movement (and of the movement of other gas-phase species) may be accounted for by specifying the "tortuosity" of the electrode, whereby the effective path length for transport is the product of the geometric distance and the tortuosity. The (perhaps position dependent) ratio of gas-filled cross-sectional area to geometric cross-sectional area $\epsilon(z)$ defines the relative "openness" of the electrode.

Transfer of mass between phases takes place at areas of gas-liquid interface. If current is being produced in the vicinity of a portion of interfacial area, there will be a net transfer of reactant gas across the interface at that area. If no current is being produced nearby, reactant equilibrium will exist between the two phases at that area, in the

sense that there will be no net transfer of reactant across the interface. In either case there may be net transfer of some other species across the interface.

The foregoing discussion leads logically to the definition of a current density based on a unit area of gas-liquid interface. The distribution of reactant gas in the gas phase can then be determined if this current per unit interfacial area can be specified and if the occurrence of gas and liquid phases in the volume under scrutiny can be described.

Expressions for the interfacial current density may be derived, but require some additional specification of electrode structure, reaction kinetics, and liquid behavior and so lose some generality. Considerable information can be had, however, without fixing the detailed interfacial current density distribution, but rather by investigating various postulatory forms of the distribution. Generally, then, this work will assume various forms for $i_i(z)$, where i_i is the interfacial current density and z the coordinate distance from the electrode surface.

Finally, we shall define an important quantity, $\xi(z)$, where $\xi(z)$ is the position-dependent quantity: interfacial area per unit geometric volume. It is this parameter that preserves the generality of this approach. It has significance regardless of whether it is considered an unspecified parameter or whether it is applied to a specific idealized picture of an electrode (e.g., the simple pore model (ref. 3), or the flooded agglomerate model (ref. 4)).

The situation within a "punched out" volume of electrode, with particular regard to the gas phase, can now be analyzed. Note that the molar reaction rate per unit volume is $[i_i(z)/n_R f]\ \xi(z)$ where n_R is equivalents per mole, and that the total current produced by the volume is

$$I_{vol} = \int_0^L i_i(z)\,\xi(z)\,\delta A\,dz$$

where L is the depth of electrode in which there exists some gas phase and δA is the geometric cross-sectional area of the cylindrical volume. (All symbols are defined in appendix A.)

EQUATIONS DESCRIBING BEHAVIOR

To completely describe mathematically the transport processes in the gas phase one needs (1) a continuity or conservation equation for each species, (2) expressions relating flux and concentration of each species, (3) an equation of state for the mixture, (4) an

equation of motion or momentum conservation, and (5) an equation of conservation of energy.

The general form of the continuity equations to be used herein is

$$\frac{-\partial(N_i \epsilon)}{\partial z} - \eta_i(z)\,\xi(z) = \frac{\epsilon\,\partial C_i}{\partial t} \tag{1}$$

where N_i is the z-direction flux, based on gas-filled area, of species i with respect to fixed coordinates; η_i is the rate in moles per unit area of interface at which species i is transferred into the liquid phase; and C_i is the gas-phase concentration of species i. This expression embodies the assumption that the net transfer of material out of the volume through its sides is negligible; that is, reactants and products are exchanged with the surroundings only in the positive or negative z-directions.

Equation (1) is then an effectively one-dimensional expression; variations from region to region in the electrode may be accounted for by suitable boundary conditions at the electrode surfaces.

The fluxes and concentrations of the various species are related by the so-called Stefan-Maxwell equations (ref. 5, p. 570). These consist of an equation of the following form written for each of the n species:

$$\frac{1}{\tau}\frac{\partial X_i}{\partial z} = \sum_{j=1}^{n} \frac{1}{C_T D_{ij}} (X_i N_j - X_j N_i) \tag{2}$$

where X_j is the mole fraction of the j^{th} component, C_T is the total concentration, τ is the electrode tortuosity described earlier, and D_{ij} the diffusivity of the pair i-j in a binary mixture. This expression embodies the assumptions that the gas phase is an ideal-gas mixture and that transport takes place by ordinary diffusion (and possibly convection) only. The utility of the Stefan-Maxwell equations lies in the fact that they express the fluxes in multicomponent systems in terms of a quantity $(C_T D_{ij})$ that may be calculated from binary system data or correlations. Furthermore this quantity is independent of both pressure and relative composition for ideal gases at low pressures (ref. 5, p. 510). Note that the equations reduce to the usual form for the binary situation, and that the use of the Stefan-Maxwell equations requires that the equation of state be the ideal-gas law.

The equation of motion may be written in the following form, which is known as Darcy's Law. Gravitational effects are neglected.

$$V_o = -\frac{k}{\mu}\frac{\partial P}{\partial z} \tag{3}$$

where V_o is the so-called superficial velocity - the volume rate of flow through a unit cross-sectional area; μ is the viscosity of the mixture; and k is the permeability of the porous material. The volume rate of flow per unit gas-filled area is given by $1/\epsilon$ times equation (3). Equations (1) and (2) may be solved for the gas-phase compositions without need of equation (3) if the species fluxes N_i are known. This is the approach to be taken in the remainder of this work and thus equation (3) will not be dealt with further. In a rigorous analysis, however, equation (3) would be solved simultaneously with equations (1) and (2) to give the net convective mass flow.

An equation of energy in steady-state form may be written for the gas-filled portion of the control volume:

$$-\frac{d}{dz}\left[\epsilon\left(-k_g\frac{dT_g}{dz}+\sum_i N_i h_i\right)\right] + \xi(z)Q(z) = 0 \tag{4}$$

where k_g is the thermal conductivity of the gas mixture, T_g the local gas temperature, h_i the molar enthalpy of the species i, and Q(z) the rate at which energy is transferred across a unit area of gas-liquid interface. This expression assumes that kinetic and potential energy effects are negligible and that the z-direction energy flux is made up of ordinary conductive and convective components only.

This work will not be concerned with solving expression (4). As a rule, temperature gradients do not directly affect mass transport, althrough the converse is not true, as evidenced by the appearance of the species fluxes N_i in equation (4). Equations (1) to (3) are written to show temperature dependence only in the physical properties, and these can be evaluated at the mean or nominal temperatures chosen without too much error.

A further assumption is made regarding these descriptive expressions in the remainder of this work - all time-dependent terms are negligible. This means that the example solutions presented cannot describe situations that are clearly transient (e.g., behavior immediately after a change in current drawn). They can, however, be applied to "slow" processes, such as the gradual buildup of inert species in the gas phase, by considering the process to proceed as a succession of pseudo-steady-states.

Finally, in all the specific cases considered in the following sections the quantity $\xi(z)$ is assumed to be constant over the range $z = 0$ to $z = L$. In physical terms this means that the cross-sectional area available for gas-phase transport is constant throughout the region of the electrode in which the gas phase is present.

If the liquid in this region is confined to small pores within the solid particles and/or thin films upon the particles, then ϵ may be identified with the so-called macroporosity of the electrode. If, however, considerable amounts of liquid are present in partially liquid-filled large interparticle pores and consequent menisci, the available area for gas transfer will be less than that given by the electrode macroporosity, since that property is based on dry electrode structure.

Variations in liquid distribution may be investigated if desired by postulating forms for the z-dependency of ϵ and solving the pertinent equations by numerical methods.

The remainder of this work is concerned with the analysis of various operating situations using the expressions developed in this section. The major goals in each case are (1) to assess the validity of the assumption of constant reactant partial pressure throughout the gas phase, and (2) to investigate the distribution of inerts (if present) in the gas phase in the electrode.

ANALYSIS OF SPECIFIC SITUATIONS - THE ANODE AT WHICH WATER IS BEING REMOVED

Here the gas phase is assumed to be made up of hydrogen gas, water vapor, and an inert impurity. The composition of the gas in the gas cavity immediately above the control volume is assumed to be known. It should be borne in mind that the gas cavity composition may differ from place to place and that the analysis of a single volume increment may not represent the conditions over an entire electrode.

For hydrogen, integration of equation (1) yields

$$N_{H_2} = \frac{I_{vol}}{2f\,\delta A\,\epsilon} - \frac{1}{\epsilon}\int_0^z \eta_{H_2}\,\xi\,dz$$

Recall that the molar reaction rate of hydrogen perunit volume is equal to $i_i\xi/2f$. At steady state this reaction rate per unit volume may be set equal to the rate of interphase transfer of H_2 per unit volume. The two rates will be unequal only if there exists considerable z-direction transport of dissolved hydrogen in the liquid phase, an unlikely circumstance because of the very low solubility-diffusivity product of H_2 in electrolyte solutions.

Thus $\eta_{H_2} = i_i/2f$. And from the preceding equation

$$N_{H_2} = \frac{I_{vol}}{2f\,\delta A\,\epsilon} - \frac{1}{2f\epsilon}\int_0^z i_i \xi\, dz \tag{5}$$

If water vapor is being transported in the gas phase within the electrode, equation (1) may be integrated to yield

$$N_{H_2O} = -\frac{1}{\epsilon}\int_0^z \eta_{H_2O}\xi\, dz - \frac{I_{vol}}{2f\,\delta A\,\epsilon} \tag{6}$$

If the impurity solubility is assumed to be negligible, the impurity continuity equation (eq. (1)) becomes simply $N_I = 0$.

Taking advantage of the fact that $X_{H_2O} = 1 - X_{H_2} - X_I$, and since $N_I = 0$, the Stefan-Maxwell equations may be written (from eq. (2)):

$$\frac{1}{X_I}\frac{dX_I}{dz} = \frac{\tau}{C_T D_{I\text{-}H_2}}\left(N_{H_2} + \theta N_{H_2O}\right) \tag{7}$$

and

$$\frac{dX_{H_2}}{dz} - X_{H_2}\frac{\tau}{C_T D_{H_2O\text{-}H_2}}\left(N_{H_2} + N_{H_2O}\right) = -\frac{\tau}{C_T D_{I\text{-}H_2}} N_{H_2}\left[\varphi + X_I(1 - \varphi)\right] \tag{8}$$

where

$$\theta = \frac{D_{I\text{-}H_2}}{D_{I\text{-}H_2O}}$$

$$\varphi = \frac{D_{I\text{-}H_2}}{D_{H_2O\text{-}H_2}}$$

Now, if the distributions of current density, interphase water transfer, relative gas-filled cross-sectional area, and active interfacial area are known (along with the required physical properties), the integrals in equations (5) and (6) may be evaluated,

equations (5) and (6) substituted in equations (7) and (8), and equations (7) and (8) solved for $X_I(z)$ and $X_{H_2}(z)$.

If the distributions are unknown, valuable information can be gained by postulating various forms of i_i, η_{H_2O}, and ξ which appear capable of describing the situation in a particular electrode or under a particular operating condition. In the following pages three cases of this sort are considered. The relation between each case and actual operating modes will be discussed and the general conclusions which may be drawn will be pointed out.

Case A

Essentially all the current is produced at or very near the bottom of the control volume. Likewise, all interphase transfer of H_2O takes place approximately at the bottom of the volume.

The gas-phase transport in the volume is then an equimolar countercurrent diffusion process. The situation described here is approached in nonwetting electrodes or in partially wetting electrodes operating in a "dried-out" condition.

Mathematically,

$$N_{H_2} = \frac{I_{vol}}{2f\,\delta A\,\epsilon} = -N_{H_2O}$$

and thus for a "pure" gas phase (i.e., $X_I = 0$), equation (8) yields

$$X_{H_2}(z) = X_{H_2}^{gc} - J\frac{z}{L} \tag{9}$$

where $X_{H_2}^{gc}$ is the mole fraction of hydrogen in the gas cavity (at $z = 0$) and

$$J = \frac{\tau I_{vol} L}{2fC_T D_{H_2O\text{-}H_2}\,\epsilon\,\delta A} \tag{10}$$

This quantity J will appear in all cases (as will θ and φ if impurities are present) and is of prime importance in characterizing the gas phase. Note that the quantity $I_{vol}/\delta A$ is equivalent to the apparent electrode current density.

In this case the composition change with z is directly proportional to the magnitude of J. For example, the composition change from top to bottom of the volume is (from eq. (9))

$$X_{h_2}^{gc} - X_{H_2}(L) = J \tag{11}$$

If the gas phase contains inert impurities, their distribution may be had by solving equation (7), yielding

$$X_I(z) = X_I^{gc} \exp\left[\frac{1}{\varphi}(1 - \theta)J\frac{z}{L}\right] \tag{12}$$

The substitution of this expression into equation (8) has the effect of adding another term to the expression for the reactant mole fraction, that is, now

$$X_{H_2}(z) = X_{H_2}^{gc} - J\frac{z}{L} + X_I^{gc}\left(\frac{1 - \varphi}{1 - \theta}\right)\left\{1 - \exp\left[\frac{1}{\varphi}(1 - \theta)J\frac{z}{L}\right]\right\} \tag{13}$$

Also,

$$X_{H_2}^{gc} - X_{H_2}(L) = J + X_I^{gc}\left(\frac{1 - \varphi}{1 - \theta}\right)\left\{\exp\left[\frac{1}{\varphi}(1 - \theta)J\right] - 1\right\} \tag{14}$$

Values of θ and φ at two temperatures are given in table I for four likely impurities. For ideal-gas mixtures at low pressures, θ and φ are independent of composition and total pressure (see appendix B for calculation of diffusivities).

In case A, it was postulated that current production takes place at the bottom of the volume. In this situation the mole fraction (or partial pressure) of H_2 at z=L should be as high as possible. The higher the partial pressure the greater the concentration of dissolved hydrogen in the liquid phase, and thus the lower the electrode polarization for a given current density.

The partial pressure of water vapor at the bottom of the volume is also of interest, since it is related to the concentration of the electrolyte "beneath" it. For example, if the gas cavity composition is fixed, at steady-state the partial pressure of H_2O at z=L must be that which allows vapor-phase transport of the stoichiometric amount of H_2O out of the electrode. And this dictates what the concentration of the liquid electrolyte immediately below must be (for a given temperature).

Evaluation of equation (12) at z=L and equation (14), together with the relation

$X_I + X_{H_2O} + X_{H_2} = 1$, yields the composition of the gas phase immediately above the electrolyte. Figures 2(a) to (c) give example results for the four impurities in table I. The temperature was chosen to be 343 K and the H_2O vapor mole fraction in the gas cavity above the volume is constant at 0.15. The $J = 0$ points correspond to open-circuit, static equilibrium situations and thus represent the constant gas cavity composition associated with each curve. Note that figure 2(b) holds for both N_2 and Ar and that all three figures are for J ranging from 0 to 0.2.

Although the three figures are rather different in appearance, one important similarity exists - for a given gas cavity composition and J the value of X_{H_2} is nearly the same regardless of the impurity species. This is because of the relative ease with which H_2 diffuses through gas mixtures. The binary diffusion coefficients of H_2 with another gaseous species are relatively high and relatively insensitive to the identity of the other gas. This effect is shown clearly in figure 3 wherein $X_{H_2}(z=L)$ is plotted as a function of J for the several values of X_I^{gc}. Here $X_{H_2}(L)$ is essentially identical for CH_4, N_2, and Ar, the exception being He, which shares with H_2 the ability to diffuse with relative ease.

Although the mole fraction of H_2 in the gas phase at $z=L$ is more or less independent of impurity species, the mole fraction of H_2O is not. In fact, the highly species-dependent balance between H_2O and impurity accounts for the marked difference in appearance of the three parts of figure 2. In general, the higher the value of θ (see table I) the greater the concentration of water vapor at $z=L$ for a given gas cavity composition and J-value. This is an important relation because it gives information about the relative dilution or concentration required of the electrolyte at a given steady-state condition. Thus, if methane is introduced into a formerly pure gas phase where the partial pressure of H_2O in the gas cavity is controlled, the electrolyte must be considerably diluted if the same amount of current is to be produced (and product water removed) on a steady-state basis. But introduction of helium, on the other hand, actually leads to a slightly more concentrated liquid electrolyte.

The results of this case have been discussed in some detail - not because of its particular importance but rather to illustrate the sort of information yielded by solutions of the describing equations. The following cases are considered in somewhat less detail.

Case B

The anode of case A was operating quite inefficiently from the standpoint of catalyst utilization. Now consider the other extreme - a cell where current is produced throughout the control volume at a constant rate per unit volume. The transfer of H_2O into the

gas phase will be assumed to take place at the same rate and this can be seen to be a situation where transport in the gas phase is again through equimolar countercurrent diffusion. A cell behaving in this manner would have to have (1) an electrolyte with very high conductivity, (2) very good liquid-phase mass transport characteristics, and (3) large cross-sectional area liquid paths between points in the anode and points in the bulk liquid.

Mathematically, for this case

$$\frac{i_i}{2f}\,\xi = -\,\eta_{H_2O}\xi = \text{Constant} = \frac{I_{vol}}{2f\,\delta A\,L}$$

and so from equations (5) and (6)

$$N_{H_2} = \frac{I_{vol}}{2f\,\delta A\,\epsilon}\left(1 - \frac{z}{L}\right) = -\,N_{H_2O}$$

For a "pure" gas phase, solution of equation (8) yields

$$X_{H_2}(z) = X_{H_2}^{gc} - J\frac{z}{L} + \frac{J}{2}\left(\frac{z}{L}\right)^2 \tag{15}$$

and now

$$X_{H_2}^{gc} - X_{H_2}(L) = \frac{J}{2}$$

The distribution of any impurities present is now (from solution of eq. (7))

$$X_I(z) = X_I^{gc}\exp\left\{\frac{1}{\varphi}(1-\theta)\left[J\frac{z}{L} - \frac{J}{2}\left(\frac{z}{L}\right)^2\right]\right\} \tag{16}$$

and substitution of this into equation (8) yields the solution for H_2 distribution in the presence of inerts:

$$X_{H_2}(z) = X_{H_2}^{gc} - J\frac{z}{L} + \frac{J}{2}\left(\frac{z}{L}\right)^2 + X_I^{gc}\left(\frac{1-\varphi}{1-\theta}\right)\left\{1 - \exp\left(\frac{1}{\varphi}(1-\theta)\left[J\frac{z}{L} - \frac{J}{2}\left(\frac{z}{L}\right)^2\right]\right)\right\} \tag{17}$$

Equations (15) to (17) can be seen to be identical to equations (9), (12), and (13), except that where J(z/L) appeared previously, the quantity

$$J\frac{z}{L} - \frac{J}{2}\left(\frac{z}{L}\right)^2$$

is now found. The analog of equation (14) is now

$$X_{H_2}^{gc} - X_{H_2}(L) = \frac{J}{2} + X_I^{gc}\left(\frac{1-\varphi}{1-\theta}\right)\left\{\exp\left[\frac{1}{\varphi}(1-\theta)\frac{J}{2}\right] - 1\right\} \tag{18}$$

Now since current is being produced throughout the volume, the composition at z=L is no longer of prime importance. Comparison of the corresponding figures, however, shows that the composition change from z=0 to z=L will be only about half as great in this case, compared to case A, for the same gas cavity composition and J value. Figure 4 shows the composition at z=L from equations (16) and (18) for N_2. Compare this figure to figure 2(b).

In this case the integrated mean composition is more indicative of the electrochemical behavior of the electrode than is the composition at z=L. From equation (16)

$$\overline{X}_I = \frac{1}{L}\int_0^L X_I^{gc} \exp\left\{\frac{1}{\varphi}(1-\theta)\left[J\frac{z}{L} - \frac{J}{2}\left(\frac{z}{L}\right)^2\right]\right\} dz$$

This expression may be rewritten

$$\frac{\overline{X}_I}{X_I^{gc}} = \int_0^1 \exp\left[\psi \cdot (2u - u^2)\right] du \tag{19}$$

where $u = z/L$ and $\psi = 1/\varphi(1-\theta)J/2$.

The expression (from eq. (17)) for the mean mole fraction of H_2 becomes

$$\overline{X}_{H_2} = X_{H_2}^{gc} - \frac{1}{3}J + X_I^{gc}\left(\frac{1-\varphi}{1-\theta}\right) - \left(\frac{1-\varphi}{1-\theta}\right)\overline{X}_I \tag{20}$$

and the mean mole fraction of H_2O is given by

$$\overline{X}_{H_2O} = 1 - \overline{X}_I - \overline{X}_{H_2} \tag{21}$$

Equation (19) can be easily integrated numerically to give X_I, and the mean composition of the gas phase can then be found. Figures 5(a) to (c) give the mean compositions of the gas phase under operating conditions paralleling case A.

By comparing figures 2 and 5, it can be seen in general that for a given impurity the composition in case B is equivalent to the composition at a lower J-value in case A. In other words, the curves for a given impurity in case B are essentially identical with the lower portions of the case A curves. Therefore, the remarks made earlier regarding the dilution and concentration of the electrolyte apply in this case, although now it is the mean concentration of all the liquid in the electrode about which the figures yield information.

Before extracting any generally applicable conclusions it would be well to investigate a case where the gas-phase diffusion is not equimolar and countercurrent throughout the electrode. Deviations from equimolar countercurrent behavior occur if the rate of evaporation of H_2O per unit volume is different from the rate of current production per unit volume.

Case C

Let the current be produced at a constant rate throughout the control volume, as in case B. Now, however, it will be assumed that all the interphase transport of H_2O takes place at or very near the $z = 0$ plane. Thus, the hydrogen now diffuses through a quiescent mixture of H_2O (and inert). This is an extreme case but it serves to bracket real situations and this condition might be approached in a cell under certain circumstances. This anode would necessarily have the properties described in case B and would, in addition, require that the H_2O produced in the upper half of the volume diffuse through the electrolyte to the $z = 0$ surface before evaporating. (This is the simplest way of meeting the conditions of this case while satisfying the steady-state stoichiometric requirement that one-half the water produced at the anode be transported via the liquid phase to the cathode while the other half is removed continuously.)

Mathematically, $\eta_{H_2O}\xi = 0$ and $N_{H_2O} = 0$. Note that equation (1) pertains to this case rather than equation (6) since there is no H_2O vapor transport within the electrode.

As in case B

$$\frac{i_i \xi}{2f} = \text{Constant} = \frac{I_{vol}}{2f\,\delta A\,L}$$

and

$$N_{H_2} = \frac{I_{vol}}{2f\,\delta A \epsilon}\left(1 - \frac{z}{L}\right)$$

This yields from equation (7)

$$X_I = X_I^{gc} \exp\left\{\frac{J}{\phi}\left[\frac{z}{L} - \frac{1}{2}\left(\frac{z}{L}\right)^2\right]\right\} \tag{22}$$

and the expression for the H_2 distribution from equation (8) is

$$X_{H_2} = 1 - X_I^{gc} \exp\left\{\frac{J}{\varphi}\left[\frac{z}{L} - \frac{1}{2}\left(\frac{z}{L}\right)^2\right]\right\} - X_{H_2O}^{gc} \exp\left\{J\left[\frac{z}{L} - \frac{1}{2}\left(\frac{z}{L}\right)^2\right]\right\} \tag{23}$$

This expression also is applicable when the gas phase is pure, that is, when $X_I^{gc} = 0$.

Figure 6 shows the composition at $z = L$ with N_2 as the impurity. This figure may be compared with figures 2(b) and 4. In this case the mole percent of water vapor is very nearly constant, varying only very slightly with position and J-value.

Equations (22) and (23) may be integrated numerically to get the mean composition of the gas phase. Figure 7 shows the result for the, by now familiar, example conditions. The behavior is approximately the same for CH_4, N_2, or Ar since their respective φ-values are nearly the same. Again, the mole fraction H_2O is nearly unchanging. The mean composition when He is the impurity varies only a few mole percent from $J = 0$ to $J = 0.2$ and would be superimposed on the low-J-value portions of the curves of figure 7.

In contrast to cases A and B, the mole fraction of impurity now increases as J increases. This is to be expected, however, because now the net flux of mass in the pore is proportional to the current density and thus increasing amounts of inerts are carried into the pore with increased reactant fluxes.

Discussion of Anode Results

Three modes of operation have been investigated for a porous fuel-cell anode with hydrogen fuel and an aqueous electrolyte. These three cases represent extremes which bracket the situations found in most existing anodes.

Most practical anodes are completely or partially hydrophilic and thus liquid may be distributed fairly evenly throughout the electrode. Except possibly under optimum conditions, however, there are appreciable electrical potential gradients in the z-direction. And thus while current generation is not confined to the very bottom of the electrode, neither is it likely to be distributed evenly throughout the electrode.

Although the rate at which H_2O is evaporated across an area of gas-liquid interface should be proportional to the amount of current generated in the vicinity, the ratio of interphase H_2O transfer to current density is probably somewhat greater at low z-values than at values of z near L.

It should also be recognized that in an actual fuel cell the pattern of gas flow in the gas cavity above the anode may be such as to force different portions of the anode into different modes of operation. If, for instance, a dry stream of reactant is used to remove product water vapor, the portion of electrode near the gas cavity inlet may be considerably drier than the portion near the exit. The region near the inlet may thus be more nearly represented by case A, while the region near the exit has perhaps more the character of case B. Also, if the gas flow is clearly directional for some length the gas cavity composition will vary along this length, becoming depleted of reactant in the direction of flow.

It is clear then that a rigorous mathematical description of a fuel-cell anode in operation requires simultaneous solution of kinetics, gas- and liquid-phase transport, and gas cavity flow. The idealized cases A to C offer an alternate means of gaining generally applicable conclusions, however, by virtue of certain similarities between them.

In each case, expressions have been derived for a gas-phase composition which is representative of the electrode. In case A it is the composition immediately above the gas-liquid interface, and in cases B and C the integrated mean composition in the electrode. It can be seen that in each case the same three parameters J, θ, and φ appear and that their effects are the same.

Thus, regardless of the detailed mode of operation of an anode, the state of the gas phase within the anode and the effect of this gas phase on performance can be characterized if the values of J, θ, and φ are known.

The following conclusions apply. They are first listed, and then discussed at length below:

(1) The larger the value of J the more position-dependent is the partial pressure of reactant.

(2) If inert impurities are present, the higher the value of θ, the greater the position-dependency of the water vapor partial pressure.

(3) If inerts are present, the higher the value of φ the more likely is the impurity to be distributed equally throughout the gas phase. This conclusion is related to conclusion (2) and thus will not be discussed separately.

With regard to conclusion (1), it can be seen from the figures that case A shows the greatest variations in composition and so it may be used as a limiting case in testing values of J.

More specifically, if J is less than 0.05, the mole percent of H_2 should be within 6 mole percent of the gas cavity value everywhere in the electrode regardless of inerts. The range $0 \leq J \leq 0.05$ does in fact encompass most practical electrodes operating at current densities of less than 1 ampere per square centimeter, and so in most cases the assumption of constant reactant partial pressure in the anode is a good one. High current density, relatively closed structures (high value of τ/ϵ), or low temperatures (which decrease $D_{H_2O\text{-}H_2}$) may, however, increase J.

Conclusions (2) and (3) also deserve a more detailed discussion. If the gas phase is pure, it is obvious that the decrease in mole percent H_2 from the gas cavity value will equal the increase in mole percent of H_2O vapor. The situation is apparently more complicated if inerts are present. Although in every case the characteristic composition shows an increase in water vapor with increasing J, the magnitude of the increase (from the gas cavity composition) is highly dependent on θ, that is, the impurity species. With the exception of case C, the concentration gradient of water vapor at steady-state is determined by the amount of water vapor which must be transported from the electrode interior to the gas cavity and by the relative ease with which this transport can take place. A large value of θ, then, may be interpreted as a propensity to impede H_2O vapor diffusion, forcing the formation of a relatively larger partial pressure gradient to transport the stoichiometrically correct amount of water vapor.

It is difficult to provide quantitative guidelines for θ-values since even CH_4 (the largest θ of the species in the examples) has little effect on a cell operating in the mode of case C. Thus, unless an anode is known to operate in a particular manner, the best course is to assume its behavior is approximated by case A, and find the representative composition from figures 2 and 3. Since case A represents a worst case it yields an upper limit on the dilution effect regardless of the anode operating mode.

ANALYSIS OF SPECIFIC SITUATIONS - THE CATHODE

WITHOUT H_2O REMOVAL

Here the gas phase is assumed to consist of 0_2 gas, H_2O vapor, and an inert impurity. Again, the gas cavity composition is assumed to be known. In some situations, however, it might be preferred to specify the H_2O partial pressure at z=L, (i.e., the vapor pressure of the bulk electrolyte), and the mole fraction of inerts in the gas cavity. The equations may be solved with these boundary conditions as easily as for a known gas

cavity composition, and herein the gas cavity composition is specified merely for convenience.

The continuity equations (eq. (1)) take the forms

$$N_{O_2} = \frac{I_{vol}}{4f\,\delta A\,\epsilon} - \frac{1}{4f\epsilon}\int_0^z i_i \xi\, dz \tag{24}$$

$$N_{H_2O} = -\frac{1}{\epsilon}\int_0^z \eta_{H_2O}\xi\, dz \tag{25}$$

Note that η_{H_2O} is a positive quantity if H_2O is entering the liquid phase.

Again using the pseudo-steady-state assumption, $N_I = 0$.

The chief difference between these expressions and the corresponding expressions for the anode is that now there is no net removal of H_2O from the volume via the gas phase. Thus, equation (25) is concerned with vapor-phase transport of H_2O from one part of the volume to another.

The Stefan-Maxwell equations (eq. (2)) take forms analogous to the corresponding forms for the anode (compare with eqs. (7) and (8)):

$$\frac{1}{X_I}\frac{dX_I}{dz} = \frac{\tau}{C_T D_{I\text{-}O_2}}\left(N_{O_2} + \theta N_{H_2O}\right) \tag{26}$$

and

$$\frac{dX_{O_2}}{dz} - X_{O_2}\frac{\tau}{C_T D_{H_2O\text{-}O_2}}\left(N_{H_2O} + N_{O_2}\right) = -\frac{\tau}{C_T D_{I\text{-}O_2}} N_{O_2}\left[\varphi + X_I(1-\varphi)\right] \tag{27}$$

where now

$$\theta = \frac{D_{I\text{-}O_2}}{D_{I\text{-}H_2O}}$$

and

$$\varphi = \frac{D_{I\text{-}O_2}}{D_{H_2O\text{-}O_2}}$$

Here again the procedure is to postulate various spatial distributions of interphase transfer and to investigate the results with the aim of drawing generally applicable conclusions.

Case A

Essentially all the current is produced at or very near the bottom of the volume. The reactant gas thus is transported through a stagnant mixture of H_2O vapor and inert. This case represents a hydrophobic, or a dried-out, electrode. Thus equations (24) and (25) become

$$N_{O_2} = \frac{I_{vol}}{4f\ \delta A\ \epsilon}$$

and

$$N_{H_2O} = 0$$

Substituting these expressions into equation (26) yields the inert distribution:

$$X_I = X_I^{gc} \exp\left(\frac{J}{\varphi}\frac{z}{L}\right)$$

where

$$J = \frac{\tau I_{vol} L}{4C_T D_{H_2O\text{-}O_2} f\ \delta A\ \epsilon}$$

The J here defined is similar to the J defined for the anode with $4C_T D_{H_2O\text{-}O_2}$ now appearing instead of $2C_T D_{H_2O\text{-}H_2}$. Because $D_{H_2O\text{-}O_2}$ is only about 1/4 $D_{H_2O\text{-}H_2}$ for a given temperature, J for the cathode is about twice the magnitude of J for the anode for identical geometric factors and current densities.

Equation (27) may be solved for the reactant distribution:

$$X_{O_2}(z) = 1 - X_I^{gc} \exp\left\{\frac{J}{\varphi}\frac{z}{L}\right\} - X_{H_2O}^{gc} \exp\left\{J\frac{z}{L}\right\} \tag{28}$$

Note that since there is no transport of water, vapor, the parameter θ does not appear.

The most interesting feature here is that both the water vapor and the inert tend to be present at higher concentrations at $z = L$ than at $z = 0$. For the inert in particular,

$$\frac{X_I(L)}{X_I^{gc}} = \exp\frac{J}{\varphi} \tag{29}$$

Values of φ and θ for the same impurities and temperatures as the anode values are given in table II. Figure 8 shows $X_I(L)/X_I^{gc}$ for the impurities in table II at 343 K. This "pile up" of inerts at the bottom of the volume results from the net mass flow (of reactant) in the z-direction, which carries along some of the inert.

Case B

The next case for consideration, as a contrast to case A, is the situation where the current is produced at a constant rate per unit volume for all z. As in the preceding case there is no H_2O vapor transport. The mathematical expressions for this case are identical with those in case C for the anode. Thus, equations (22) and (23) describe the gas-phase composition in this case for O_2 as the reactant as well as for H_2. Equation (22) evaluated at $z = L$ now yields

$$\frac{X_I(L)}{X_I^{gc}} = \exp\left(\frac{1}{2}\frac{J}{\varphi}\right) \tag{30}$$

And so, although the inert still tends to accumulate in the bottom of the volume, the ratio of equation (30) is equal only to the square root of the ratio in equation (29).

Case C

Here a somewhat closer approximation to reality is to let the current production increase linearly with z. Thus

$$i_i \xi = 2 \frac{I_{vol}}{\delta A\ L} \frac{z}{L}$$

Again, assuming no H_2O vapor transport, $N_{H_2O} = 0$ and from equation (24)

$$N_{O_2} = \frac{I_{vol}}{4f\ \delta A\ \epsilon} \left[1 - \left(\frac{z}{L}\right)^2\right]$$

The tendency for the majority of the current production to be near the bottom of the volume should be more pronounced in the cathode than in the anode because of reactant solubility gradients. In the anode the electrolyte in the upper region ($z < L/2$) is dilute relative to the lower region and so the gas solubility is relatively higher in the upper regions. This effect, which would tend to produce more evenly distributed current production, is reversed in the cathode; so the potential gradient, the availability of liquid species, and reactant solubility all tend to favor the lower region of the cathode.

The inert distribution from equation (26) is now

$$X_I = X_I^{gc} \exp\left\{\frac{J}{\varphi}\left[\frac{z}{t} - \frac{1}{3}\left(\frac{z}{t}\right)^3\right]\right\} \tag{31}$$

and the reactant distribution (from eq. (27))

$$X_{O_2} = 1 - X_I^{gc} \exp\left\{\frac{J}{\varphi}\left[\frac{z}{L} - \frac{1}{3}\left(\frac{z}{L}\right)^3\right]\right\} - X_{H_2O}^{gc} \exp\left\{J\left[\frac{z}{L} - \frac{1}{3}\left(\frac{z}{L}\right)^3\right]\right\} \tag{32}$$

As before it is desirable to specify the gas-phase composition at some point which is representative of the electrode as a whole. In this case, since current production is greater near the bulk electrolyte than near the bulk gas (i.e., greater for larger z/L), this composition should be a weighted rather than a simple mean. To this end the composition at $z/L = \sqrt{1/2}$ was chosen, which represents the point at which one-half the total current has been produced. Figure 9 shows this composition for N_2 as the inert at 343 K. The mole fraction of H_2O vapor in the gas cavity is held at 0.10. Note that,

because of the similarity of φ-values, this also represents (to within a few percent) the situation when CH_4 or Ar is the impurity.

It is also instructive to use the results of this case to compare a "pure" oxygen cathode to an air cathode. Figure 10 shows the mole fraction 0_2 at $z/L = \sqrt{1/2}$ for the two situations with $X_{H_2O} = 0.1$ and $T = 343$ K. This figure illustrates the fact that the more inert present, the greater is the magnitude of $\partial X_{0_2}/\partial J$. Also, the larger the mole fraction inert, the steeper the oxygen mole fraction gradient is in the z-direction at a given J.

Case D

As a last example, consider a circumstance where a portion of the water required in the current production reaction is evaporated into the gas phase and then recondensed in the vicinity of a reaction site. More specifically, for mathematical simplicity it is assumed that one-half the total H_2O stoichiometric requirement evaporates at or near $z = L$, is transported in the negative z-direction, and condenses at a molar rate per unit volume equal to that at which the 0_2 enters the liquid phase at all z. This is equivalent to saying that one-half the H_2O reacted at every point arrives in the vicinity through the gas phase.

Thus, $\eta_{H_2O}{}^{\xi} = i_i \xi/4f$.

Assuming the current production is linear with z as in case C, equation (24) yields

$$N_{0_2} = \frac{I_{vol}}{4f\ \delta A\ \epsilon}\left[1 - \left(\frac{z}{L}\right)^2\right]$$

and from equation (25)

$$N_{H_2O} = -\frac{I_{vol}}{4f\ \delta A\ \epsilon}\left(\frac{z}{L}\right)^2$$

Substituting these into equation (26) yields for the inert distribution

$$X_I = X_I^{gc} \exp\left\{\frac{J}{\varphi}\left[\frac{z}{L} - \frac{1}{3}(1+\theta)\left(\frac{z}{L}\right)^3\right]\right\} \tag{33}$$

Equation (27) may now be solved for the reactant distribution

$$\rho\left(\frac{z}{L}\right)\cdot X_{O_2}\left(\frac{z}{L}\right) = X_{O_2}^{gc} - \int_0^{z/L} J\left[1 - \left(\frac{z}{L}\right)^2\right] \rho\left(\frac{z}{L}\right) d\left(\frac{z}{L}\right)$$

$$- \left(\frac{1}{\varphi} - 1\right) \int_0^{z/L} J\left[1 - \left(\frac{z}{L}\right)^2\right] \rho\left(\frac{z}{L}\right) X_I\left(\frac{z}{L}\right) d\left(\frac{z}{L}\right) \qquad (34)$$

where

$$\rho = \exp\left\{-J\left[\frac{z}{L} - \frac{2}{3}\left(\frac{z}{L}\right)^3\right]\right\}$$

Both integrals on the right side of equation (34) require numerical solution.

The first integral on the right side of equation (34) gives the pure gas-phase composition. Figure 11 shows X_{O_2} for the pure gas phase at 343 K with $X_{H_2O} = 0.1$. The equivalent result from case C is represented by the dashed lines.

Consideration of figure 11 yields more information about the situations to which cases C and D pertain. Case C requires that the liquid and gas phases be in equilibrium with respect to H_2O at all values of z/L. Thus, the small variation in mole fraction H_2O in the gas phase implies a similarly small variation in liquid-phase concentration. If, on the other hand, case D describes the gas phase, the two phases are in equilibrium only at $z/L = 0$, and a very steep concentration gradient exists in the liquid in the region of $z/L = 1.0$. Figure 12 shows the required relation between the mole fraction H_2O in the gas phase and the equilibrium mole fraction associated with the liquid phase ($X^*_{H_2O}$).

The second integral in equation (34) gives the additive effect of the presence of an impurity. It can be numerically integrated without trouble, but for most purposes it can be evaluated directly by making a simplifying approximation involving the exponential terms. Combining them, the exponent may be written

$$J\left\{\left(\frac{1}{\varphi} - 1\right)\frac{z}{L} + \left(\frac{2}{3} - \left(\frac{1+\theta}{\varphi}\right)\frac{1}{3}\right)\left(\frac{z}{L}\right)^3\right\}$$

For $J \leq 0.4$ and the θ- and ϕ-values listed in table II, the magnitude of this exponent is always less than 0.15. Thus, the exponential may be closely approximated by the

quantity 1.0 plus the exponent, and the argument of the second integral thus becomes a polynomial in z/L. This is readily integrated analytically and the second term on the right side of equation (34) is thus

$$-\left(\frac{1}{\varphi} - 1\right) J X_I^{gc} \sum_{k=1}^{6} a_k \left(\frac{z}{L}\right)^k$$

where

$$a_1 = 1 \qquad a_4 = 0$$

$$a_2 = \frac{J}{2}\left(\frac{1}{\varphi} - 1\right) \qquad a_5 = \frac{1}{12}\frac{J}{\varphi}(5\varphi - 4 - \theta)$$

$$a_3 = -\frac{1}{3} \qquad a_6 = -\frac{1}{18}\frac{J}{\varphi}(2\varphi - 1 - \theta)$$

As in case C, the composition at $z/L = \sqrt{1/2}$ is chosen as representative. Figure 13 shows this composition for N_2 as impurity at 343 K.

The mole fraction 0_2 at $z/L = \sqrt{1/2}$ for pure 0_2 and for air is shown in figure 14 for the same conditions as figure 10.

Discussion of Cathode Results

A number of conceivable cathode operating modes have been investigated, this approach paralleling that used on the anode. And again, the hope is to have "bracketed" most realistically operating cathodes.

Case A represents a hydrophobic electrode; case B the other extreme with regard to wettability and efficient catalyst utilization. Cases C and D embody a linear spatial distribution of current, comparing the results with and without H_2O vapor transport.

To determine precisely whether H_2O is transported as vapor - and if so to what extent - requires additional analysis of the liquid phase in the cathode. As a first approximation, the larger the ratio of cross-sectional area in the gas phase to cross-sectional area in the liquid phase, the greater the likelihood for gas-phase transfer of H_2O. Water vapor transport should also be relatively greater at high current densities and if considerable amounts of current are produced in the upper (small z/L) regions

of the electrode. It is not valid to conclude that vapor transport predominates from the fact that $D^{\ell}_{H_2O\text{-}KOH} \ll D^{g}_{H_2O\text{-}0_2}$ since a more correct (although still not completely sufficient) comparison is $C^{\ell}_{T}D^{\ell}_{H_2O\text{-}KOH}$ against $C^{g}_{T}D^{g}_{H_2O\text{-}0_2}$, where C_T is the total molar concentration. And $C^{g}_{T}D^{g}_{H_2O\text{-}0_2}/C^{\ell}_{T}D^{\ell}_{H_2O\text{-}KOH}$ is only about 2 at 343 K.

Again it is found that the parameters J, θ, and φ characterize the gas phase. As before, the greater the value of J, the larger the partial pressure gradients in the gas phase. Also the smaller the value of φ the greater the propensity of the inert to distribute itself equally throughout the gas phase. The parameter θ is involved only if there is vapor-phase transport of H_2O, and it may be shown that the greater the value of θ the larger the partial pressure gradient of H_2O required for a given rate of H_2O vapor transfer.

It is worthwhile to note one difference between the gas phase in the anode and cathode. It can be seen from figures 8 to 10, 13, and 14 that the percent of inerts in the cathode will always be higher than that in the gas cavity regardless of the operating mode, which is not, in general, true of the anode. This is due to the fact that there is always a net flow of gas in the z-direction for low z/L values in the cathode (indeed, for all values of z/L unless H_2O vapor transport is taking place). The effect of this net flow is to carry some inerts into the electrode, where they accumulate until the partial pressure diffusion gradient built up is just sufficient to counteract the net flow effect.

To characterize, then, any cathode one should first find the value of J. If J is less than 0.1, the mean, or representative, mole percent of 0_2 in the electrode will be within about 8 mole percent of the gas cavity value, and the assumption of constant reactant partial pressure throughout the gas phase should prove adequate for most purposes regardless of inerts or H_2O vapor transport. The range $0 \leq J \leq 0.1$ encompasses most practical cathodes operating at current densities under 1 ampere per square centimeter. High current densities, closed electrode structures and low operating temperatures will, however, increase J.

If an inert is present and J is greater than 0.1 the values of φ and θ should be calculated. If ϕ is small (< 1) a considerable excess of inert in the electrode should be expected, and a large value of θ implies impeded vapor-phase H_2O transport. If these circumstances hold, the mean composition of the gas phase in the electrode can be approximated using case C or D or case A if the electrode is known to be highly hydrophobic.

SUMMARY OF RESULTS

A physical model for a fuel-cell electrode has been analysed for various sets of operating conditions. By assuming forms for the spatial distribution of interphase mass transfer, results have been obtained which yield information of general value concerning the composition of the gas phase within the electrode.

In particular, the three dimensionless parameters J, θ, and φ were found to characterize the gas phase in fuel-cell electrodes. The quantity J may be thought of as a dimensionless current density, while θ and φ are ratios of binary diffusion coefficients of the gaseous species present. The complete definition of these parameters may be found in appendix A.

The parameters are useful in estimating the effect of gas-phase conditions on fuel-cell performance although they by no means constitute a complete description of fuel-cell behavior, since electrical performance depends on a number of factors in addition to gas-phase concentration gradients. The maximum or reversible voltage may be calculated from thermodynamic considerations and depends on operating conditions of temperature, pressure, and electrolyte concentration. Performance losses, so-called polarization, arise as a consequence of irreversible processes associated with the drawing of current from a cell. One of these irreversible processes is the transport of reactants and products through the gas phase within the electrodes. Although specific values can not be assigned to polarization associated with the gas phase because of the coupled nature of transport in the cell, it is generally true that the greater the difference between the partial pressure of reactant in the bulk gas and that in the electrode, the poorer the electrical performance as compared to that theoretically obtainable. And conversely, if there is little or no partial pressure difference, performance losses must be attributed to other factors such as electrolyte resistivity, kinetic limitations and liquid-phase transport processes.

The chief utility, then, of the parameters J, θ, and φ lies in estimating the amount by which the reactant is diluted within the electrode through the setting up of gradients required to transport reactants and products and by the presence of inert gases. And these estimates are useful either as design information or as analytical tools in considerations of fuel-cell polarization.

Calculations of J, θ, and φ may be used in conjunction with the following generally applicable conclusions which emerge from the various cases considered.

1. The greater the value of J, the larger the concentration gradients within the electrode gas phase. Numerical limits have been established for the anode and the cathode which allow judgement as to whether gas-phase concentration gradients need be considered. More specifically if $J \leq 0.05$ for the anode, or $J \leq 0.1$ for the cathode, the maximum variation in reactant mole percent from top to bottom of the gas phase in the

electrode will be less than 10 mole percent.

2. If inert impurities are present, their effect on the gas phase depends on the values of θ and φ, that is, on the nature of the impurity. The larger the value of θ, the more transport of H_2O vapor is impeded. For example, if transport of H_2O vapor takes place, a given rate of water vapor transport requires a larger concentration gradient for larger magnitudes of θ.

The smaller the value of φ, the greater the likelihood that the concentration of inert in the electrode will differ from that in the gas cavity. In the cathode in particular, small φ values mean that the percent of inert in the electrode is considerably higher than in the gas cavity.

If quantitative information with regard to inert effects is required, estimates can be made from the results presented for the case judged to be most representative of the electrode in question. Alternatively, if enough is known about the electrode, the general equations can be solved in a manner similar to the cases herein discussed.

Lewis Research Center,
National Aeronautics and Space Administration,
Cleveland, Ohio, October 1, 1970,
120-34.

APPENDIX A

SYMBOLS

C_i	concentration of species i, g-mole/cm^3
C_T	total concentration, g-mole/cm^3
D_{ij}	diffusivity in binary gas mixture of species i and j, cm^2/sec
f	Farraday's constant, 9.65×10^4 A-sec/g-equivalent
I_{vol}	total current produced by electrode volume element, A
i_i	current produced per unit gas-liquid interface area, A/cm^2
J	$\tau I_{vol} L/n_R f C_T D_{R\text{-}H_2O} \epsilon\ \delta A$ (dimensionless)
k	permeability, cm^2/sec
k_g	thermal conductivity of gas mixture, cal/(cm^2)(sec)(K)
L	z-value of greatest penetration of gas phase towards bulk electrolyte, cm
N_i, N_j	flux of species i or j in the z-direction, g-mole/(cm^2)(sec)
n_R	equivalents per gram-mole of reactant
P	total pressure, A
Q	energy flux, cal/(sec)(cm^2)
T_g	gas temperature, K
t	time, sec
V_o	superficial velocity - volume rate of flow through unit cross-sectional geometric area, cm^3/sec/cm^2
X_i, X_j	mole fraction species i or j (dimensionless)
z	coordinate direction normal to electrode plane surfaces; equals 0 at surface adjacent to gas cavity, cm
δA	increment of electrode surface area, cm^2
ϵ	ratio gas-filled cross-sectional area to geometric cross-sectional area (dimensionless)
η_i	flux of species i across gas-liquid interface, g-mole/(cm^2)(sec)
θ	$D_{I\text{-}R}/D_{I\text{-}H_2O}$ where subscript R refers to reactant (H_2 or 0_2) and subscript I refers to inert species (dimensionless)

μ viscosity of gas mixture, cP(g/(cm)(sec))

ξ interfacial area per unit geometric volume, cm^{-1}

ρ $\exp\left\{-J\left[\frac{z}{L} - \frac{2}{3}\left(\frac{z}{L}\right)^3\right]\right\}$ (dimensionless)

τ electrode tortuosity (dimensionless)

φ $D_{I\text{-}R}/D_{H_2O\text{-}R}$ (dimensionless)

ψ $\frac{1}{\varphi}(1 - \theta)\frac{J}{2}$ (dimensionless)

Subscripts:

I inert

R reactant

Superscripts:

gc gas cavity

g gas phase

ℓ liquid phase

APPENDIX B

GAS-PHASE DIFFUSIVITIES

Binary mass diffusivities were calculated by means of one of two expressions: reactant-impurity diffusivities from the Chapman-Enskog kinetic theory formula (ref. 5, p. 510); reactant-water-vapor and impurity-water-vapor diffusivities from an expression developed by Slattery and Bird (ref. 5, p. 505) from kinetic and corresponding states arguments.

The Chapman-Enskog formula is

$$C_T D_{AB} = \frac{2.2646\times10^{-5}\left[T_g \cdot \left(\frac{1}{M_A} + \frac{1}{M_B}\right)\right]^{1/2}}{\sigma_{AB}^2 \Omega_{D,AB}} \tag{B1}$$

where M_A and M_B are the molecular weights of the two species; σ_{AB} is one of the Lennard-Jones parameters for the mixture and is given by $\sigma_{AB} = 1/2(\sigma_A + \sigma_B)$; $\Omega_{D,AB}$ is a dimensionless function of the quantity kT/ϵ_{AB}, where k is the Boltzmann constant and ϵ_{AB} is the other Lennard-Jones parameter for the mixture and is given by

$$\epsilon_{AB} = \sqrt{\epsilon_A \epsilon_B}$$

(Values of σ_i, ϵ_i, and $\Omega_{D,AB}$ are given in reference 5 (pp. 744-746).)

The diffusivities predicted by the Chapman-Enskog formula have been found to be within 10 percent of measured values for low-pressure (< 10 atm), nonpolar gas mixtures.

The expression of Slattery and Bird with the ideal-gas law embodied as equation of state is

$$C_T D_{AB} = 4.43\times10^{-6} T_g^{4/3} \left[(P_C)_A (P_C)_B\right]^{1/3} \left[(T_C)_A (T_C)_B\right]^{-3/4} \left(\frac{1}{M_A} + \frac{1}{M_B}\right)^{1/2} \tag{B2}$$

where $(P_C)_i$ and $(T_C)_i$ are the critical pressure and temperature of species i. Values predicted by this expression are thought to be accurate to within about 10 percent for pressures under 10 atmospheres.

Numerical values for θ and φ can be calculated from

$$\theta = \frac{C_T D_{I\text{-}R}}{C_T D_{I\text{-}H_2O}}$$

$$\phi = \frac{C_T D_{I\text{-}R}}{C_T D_{H_2O\text{-}R}}$$

Equations (B1) and (B2) yield the results given in table III for the species under consideration in this report. Figure 15 shows Ω as a function of T. In all cases the temperature is in degrees Kelvin, pressure in atmospheres, and $C_T D_{AB}$ in gram-moles per centimeter-second.

REFERENCES

1. Austin, L. G.: Theories of Pourous Electrodes. Ch. 18 in Fuel Cells. NASA SP-120, 1967.

2. Breiter, Manfred W.: Electrochemical Processes in Fuel Cells. Springer Verlag New York Inc., 1969, pp. 254-270.

3. Rockett, J. A.; and Brown, R.: Theory of the Performance of Porous Fuel Cell Electrodes. Journal of the Electrochemical Society, vol. 113, no. 3, Mar. 1966, pp. 207-213.

4. Giner, J. and Hunter, C.: The Mechanism of Operation of the Teflon Bonded Gas Diffusion Electrode: A Mathermatical Model. Journal of the Electrochemical Society, vol. 116, no. 8, Aug. 1969, pp. 1124-1130.

5. Bird, R. B.; Stewart, W. E.; and Lightfoot, E. N.: Transport Phenomena. John Wiley & Sons, Inc., 1960.

TABLE I. - VALUES OF θ AND φ FOR H_2 REACTANT[a]

i	Temperature, K			
	343		473	
	θ	φ	θ	φ
CH_4	8.0	0.68	6.5	0.56
N_2	2.8	.72	2.2	.59
He	.68	1.5	.54	1.21
Ar	3.1	.78	2.4	.61

[a] $\theta = D_{I\text{-}H_2}/D_{I\text{-}H_2O}$ and $\varphi = D_{I\text{-}H_2}/D_{H_2O\text{-}H_2}$.

TABLE II. - VALUES OF θ AND φ FOR H_2 REACTANT[a]

i	Temperature, K			
	343		473	
	θ	φ	θ	φ
CH_4	2.48	0.82	2.07	0.68
N_2	.74	.75	.61	.62
He	.32	2.70	.25	2.17
Ar	.75	.72	.62	.59

[a] $\theta = D_{I\text{-}O_2}/D_{I\text{-}H_2O}$; $\varphi = D_{I\text{-}O_2}/D_{H_2O\text{-}O_2}$.

TABLE III. - EXPRESSIONS TO BE USED IN CALCULATING θ and φ

i	$C_T D_{i\text{-}H_2O}$	$C_T D_{i\text{-}H_2}$	$C_T D_{i\text{-}O_2}$
H_2	$195. \times 10^{-10} T^{4/3}$	----------	----------
O_2	$51.0 \times 10^{-10} T^{4/3}$	----------	----------
CH_4	$16.9 \times 10^{-10} T^{4/3}$	$15.0 \times 10^{-7} T^{1/2}/\Omega(T/72.2)$	$5.33 \times 10^{-7} T^{1/2}/\Omega(T/124.5)$
N_2	$51.9 \times 10^{-10} T^{4/3}$	$15.2 \times 10^{-7} T^{1/2}/\Omega(T/59.0)$	$4.62 \times 10^{-7} T^{1/2}/\Omega(T/101.8)$
He	$434. \times 10^{-10} T^{4/3}$	$26.1 \times 10^{-7} T^{1/2}/\Omega(T/19.7)$	$13.3 \times 10^{-7} T^{1/2}/\Omega(T/33.9)$
Ar	$49.0 \times 10^{-10} T^{4/3}$	$16.3 \times 10^{-7} T^{1/2}/\Omega(T/68.6)$	$4.57 \times 10^{-7} T^{1/2}/\Omega(T/118.5)$

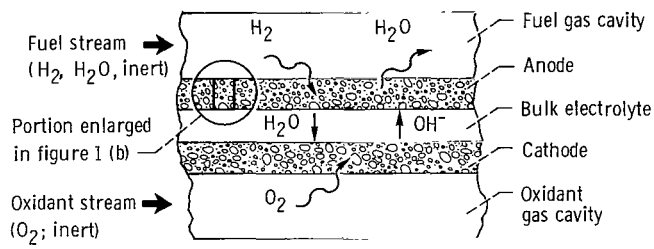

(a) Overall cell section.

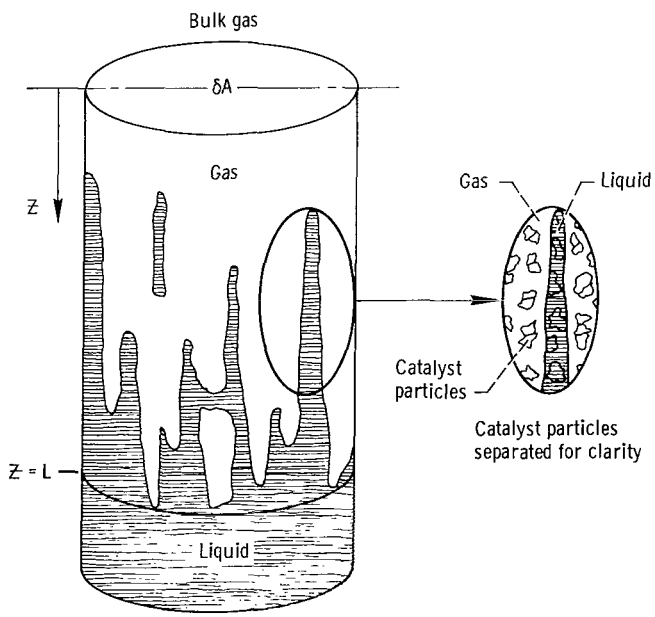

(b) Sample of electrode interior.

Figure 1. - Schematic representation of H_2 - O_2 fuel cell.

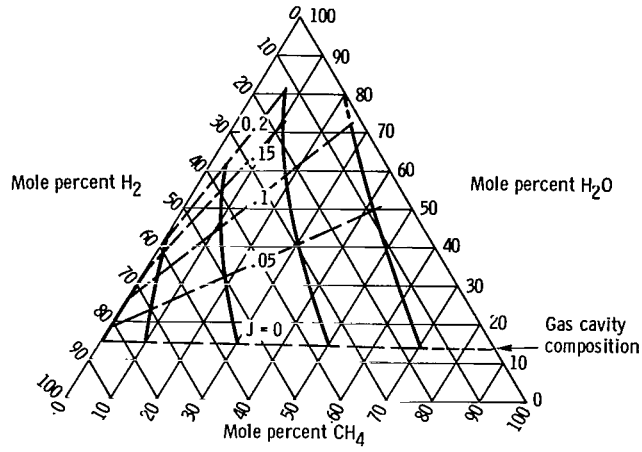

(a) Impurity, CH_4.

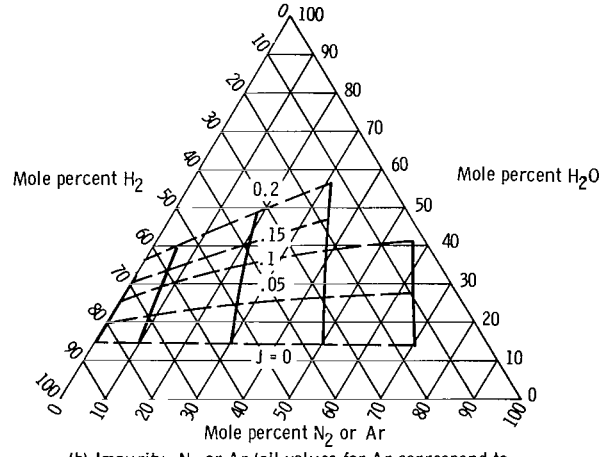

(b) Impurity, N_2 or Ar (all values for Ar correspond to those for N_2 to within 2 percent).

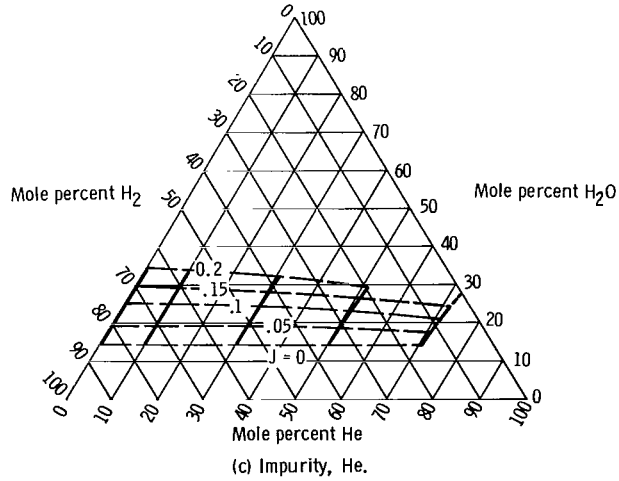

(c) Impurity, He.

Figure 2. - Gas-phase composition near bulk liquid (at z = L) - case A. Temperature, 343 K.

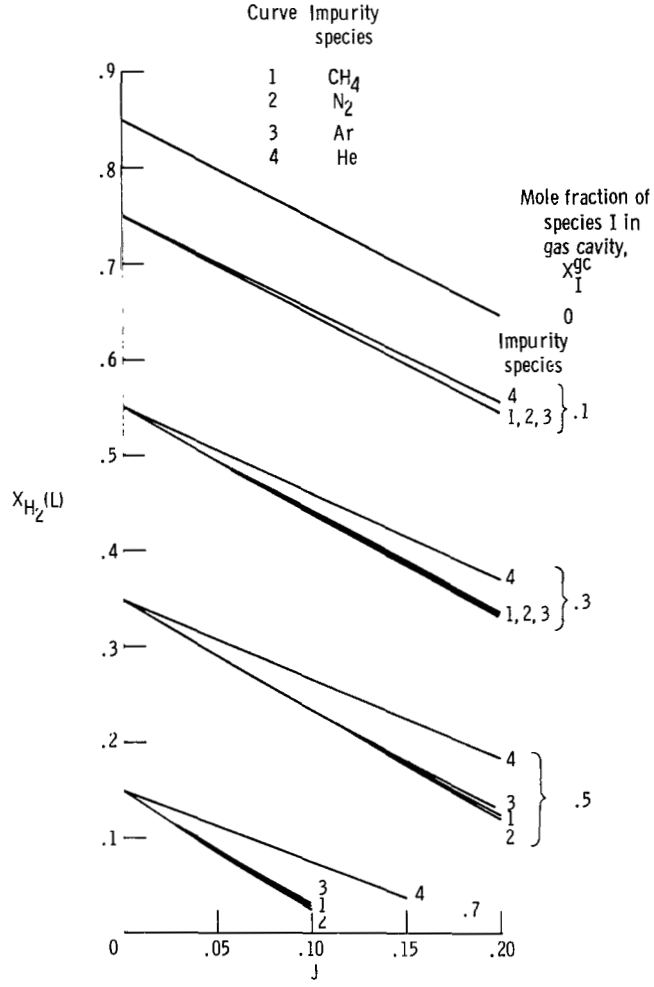

Figure 3. - Mole fraction H_2 at bottom of volume. Case A; temperature, 343 K; mole fraction of water in gas cavity, $\left(X_{H_2O}^{gc}\right) = 0.15$.

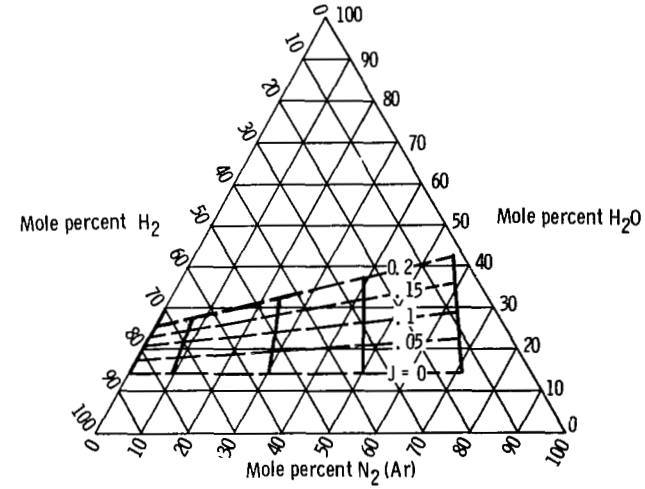

Figure 4. - Gas-phase composition near bulk liquid (at Z = L) - case B. Temperature, 343 K; impurity, N_2(Ar).

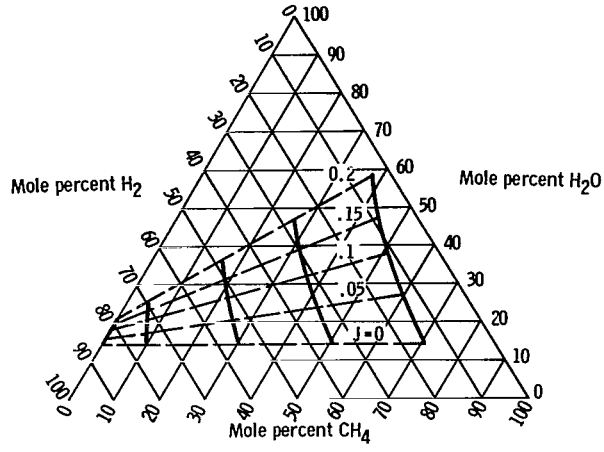

(a) Impurity, CH_4.

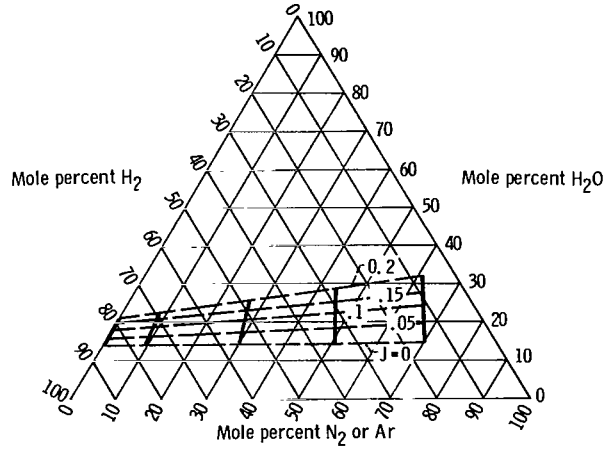

(b) Impurity, N_2 or Ar.

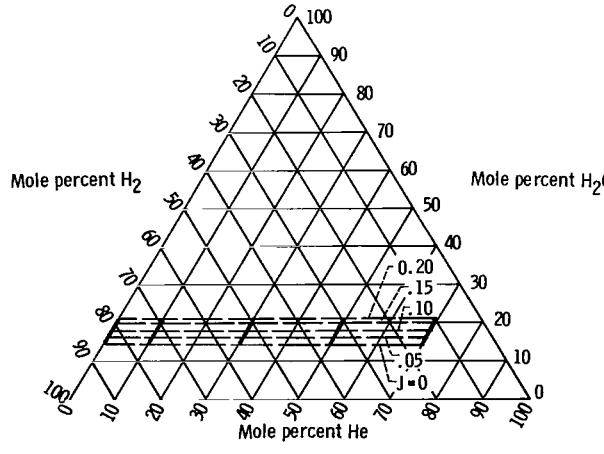

(c) Impurity, He.

Figure 5. - Mean gas phase composition - case B. Temperature, 343 K.

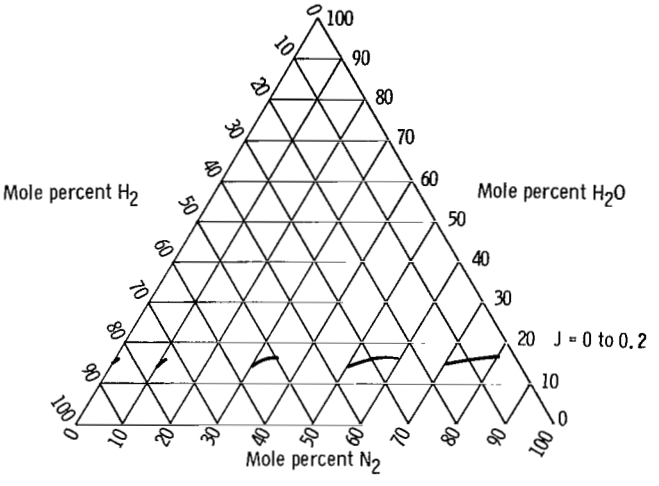

Figure 6. - Gas-phase composition near bulk liquid - case C. Impurity, N_2; temperature, 343 K.

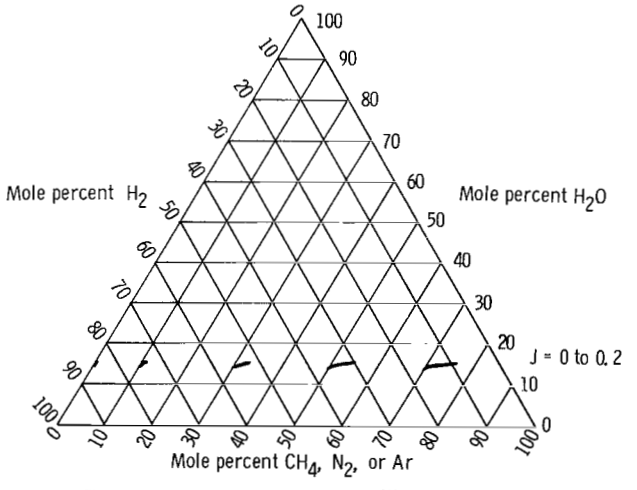

Figure 7. - Mean gas-phase composition - case C. Impurity, CH_4, N_2, or Ar; temperature, 343 K.

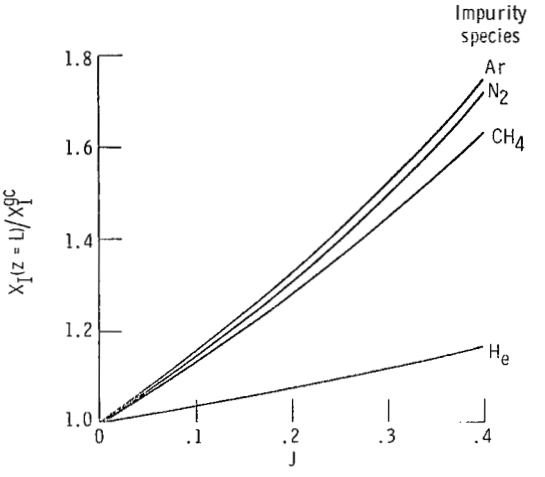

Figure 8. - Ratio of mole fraction of inert at bottom of volume to mole fraction of inert at top. Case A cathode.

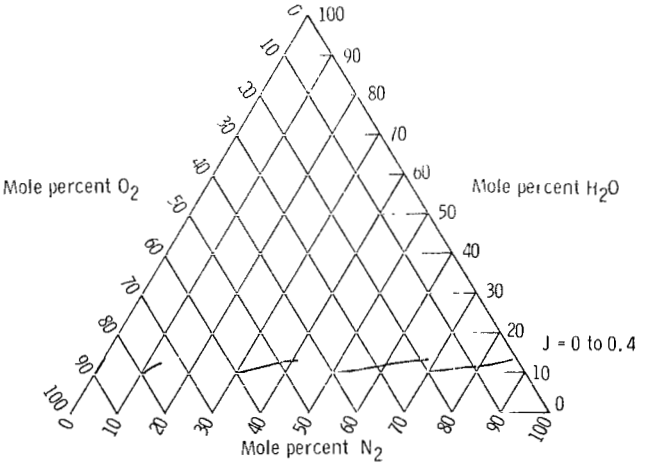

Figure 9. - Representative gas-phase composition (the composition at $z/L = \sqrt{1/2}$). Case C cathode. Impurity, N_2(Ar, CH_4); temperature, 343 K.

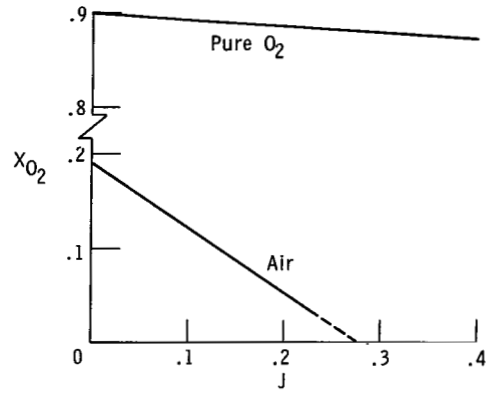

Figure 10. - Mole fraction O_2 at $z/L = \sqrt{1/2}$ ($X^{gc}_{H_2O} = 0.1$). Case C cathode; temperature, 343 K.

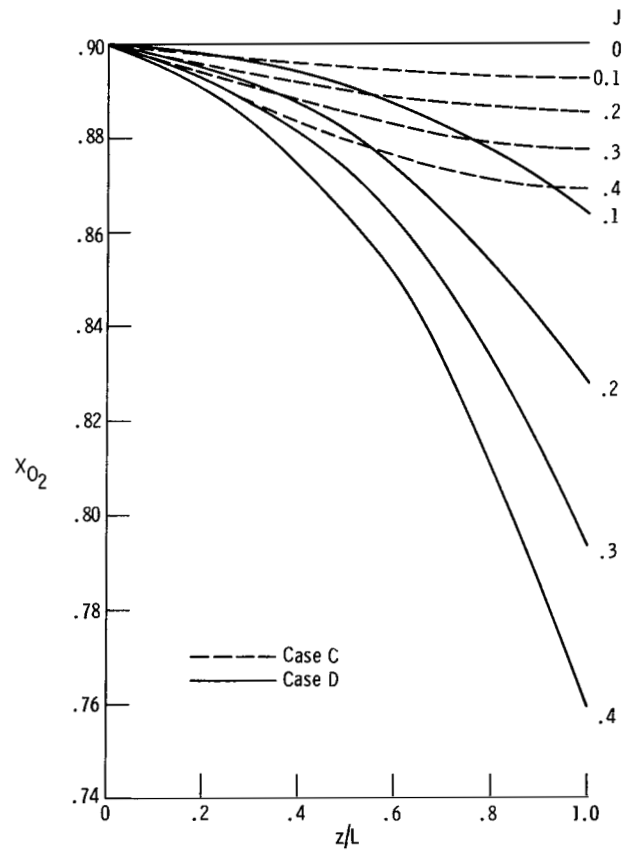

Figure 11. - Composition of pure gas phase - comparison of cases C and D. Temperature, 343 K.

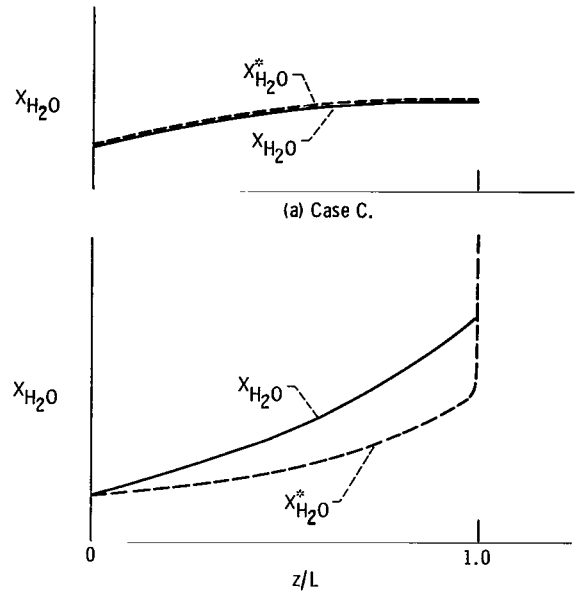

Figure 12. - Gas-phase H_2O concentration gradients. ($X^*_{H_2O}$ is the mole fraction in equilibrium with the liquid phase.)

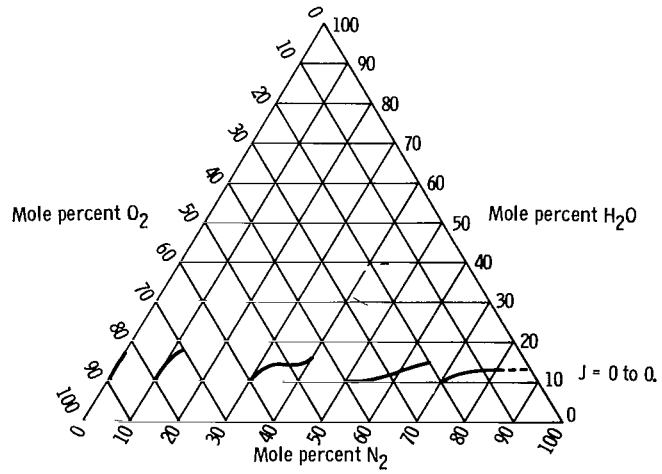

Figure 13. - Representative gas-phase composition. Case D cathode. Impurity, N_2; temperature, 343 K.

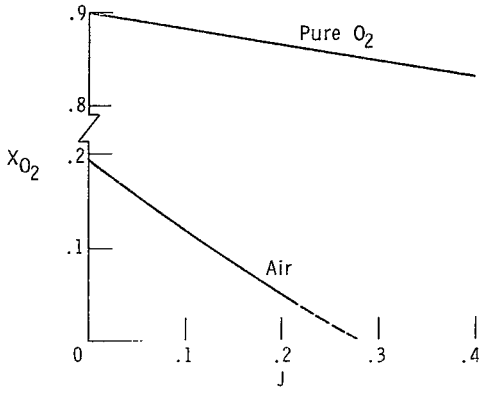

Figure 14. - Mole fraction O_2 at $z/L = \sqrt{1/2}$ ($X^{gc}_{H_2O} = 0.1$). Case D; temperature, 343 K.

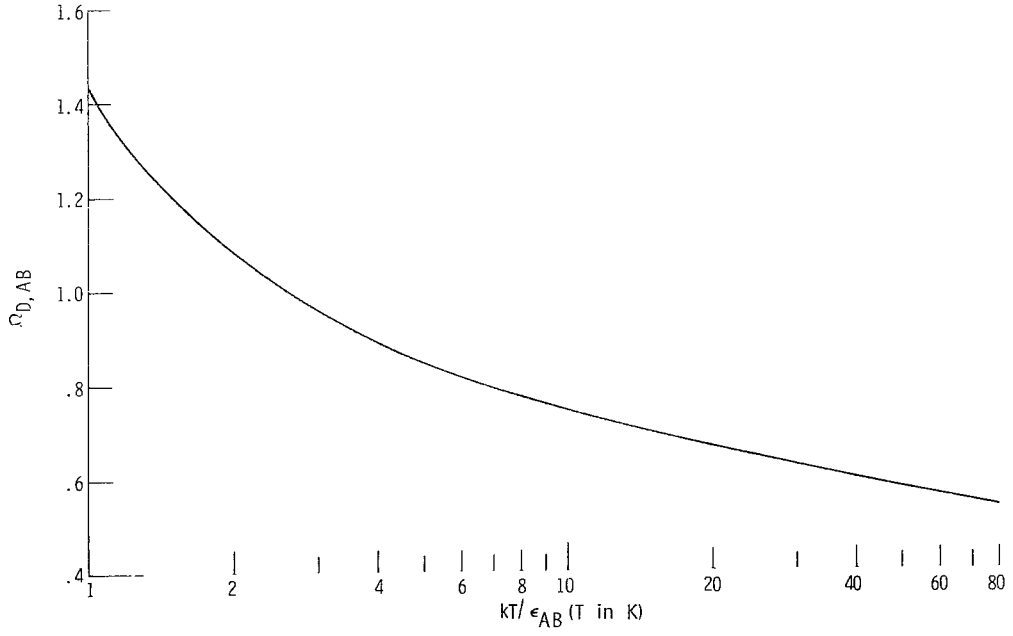

Figure 15. - Diffusivity function for use in calculating binary gas diffusivities from Chapman-Enskog theory (ref. 5, p. 746).

NASA-Langley, 1971 — 3 E-5754

"The aeronautical and space activities of the United States shall be conducted so as to contribute . . . to the expansion of human knowledge of phenomena in the atmosphere and space. The Administration shall provide for the widest practicable and appropriate dissemination of information concerning its activities and the results thereof."

—NATIONAL AERONAUTICS AND SPACE ACT OF 1958

NASA SCIENTIFIC AND TECHNICAL PUBLICATIONS

TECHNICAL REPORTS: Scientific and technical information considered important, complete, and a lasting contribution to existing knowledge.

TECHNICAL NOTES: Information less broad in scope but nevertheless of importance as a contribution to existing knowledge.

TECHNICAL MEMORANDUMS: Information receiving limited distribution because of preliminary data, security classification, or other reasons.

CONTRACTOR REPORTS: Scientific and technical information generated under a NASA contract or grant and considered an important contribution to existing knowledge.

TECHNICAL TRANSLATIONS: Information published in a foreign language considered to merit NASA distribution in English.

SPECIAL PUBLICATIONS: Information derived from or of value to NASA activities. Publications include conference proceedings, monographs, data compilations, handbooks, sourcebooks, and special bibliographies.

TECHNOLOGY UTILIZATION PUBLICATIONS: Information on technology used by NASA that may be of particular interest in commercial and other non-aerospace applications. Publications include Tech Briefs, Technology Utilization Reports and Technology Surveys.

Details on the availability of these publications may be obtained from:

SCIENTIFIC AND TECHNICAL INFORMATION OFFICE

NATIONAL AERONAUTICS AND SPACE ADMINISTRATION

Washington, D.C. 20546